Bis-Heteroleptic Ruthenium(II) Complex of a Triazole Ligand as a Selective Probe for Phosphates

ARTICLE *in* INORGANIC CHEMISTRY · JULY 2014

Impact Factor: 4.76 · DOI: 10.1021/ic5010598 · Source: PubMed

5 AUTHORS, INCLUDING:

Snehadrinarayan Khatua
North Eastern Hill University
24 PUBLICATIONS **470** CITATIONS
SEE PROFILE

Ranjan Dutta
Kangwon National University
21 PUBLICATIONS **73** CITATIONS
SEE PROFILE

Sourav Chakraborty
Indian Association for the Cultivation of Science
12 PUBLICATIONS **51** CITATIONS
SEE PROFILE

Pradyut Ghosh
Indian Association for the Cultivation of Science
108 PUBLICATIONS **2,528** CITATIONS
SEE PROFILE

Inorganic Chemistry

Article

pubs.acs.org/IC

Bis-Heteroleptic Ruthenium(II) Complex of a Triazole Ligand as a Selective Probe for Phosphates

Bijit Chowdhury,[†] Snehadrinarayan Khatua,[§] Ranjan Dutta,[†] Sourav Chakraborty,[†] and Pradyut Ghosh*[,†]

[†]Department of Inorganic Chemistry, Indian Association for the Cultivation of Science, 2A & 2B Raja S. C. Mullick Road, Kolkata 700032, India

Supporting Information

ABSTRACT: A new bis-heteroleptic ruthenium(II) complex (**1**) of 2-(1-methyl-1*H*-1,2,3-triazol-4-yl) pyridine (**L**) ligand was extensively explored for anion sensing studies. **1**$[PF_6]_2$ shows selective sensing of dihydrogen phosphate ($H_2PO_4^-$)/hydrogen pyrophosphate ($HP_2O_7^{3-}$) among halides, HCO_3^-, AcO^-, NO_3^-, ClO_4^-, HSO_4^-, OH^-, BzO^-, $H_2PO_4^-$, and $HP_2O_7^{3-}$ in acetonitrile. Enhancement of emission intensity of **1**$[PF_6]_2$ along with a 10 nm red shift of the emission maximum is observed in the presence of $H_2PO_4^-$/$HP_2O_7^{3-}$ selectively. The photoluminescence (PL) titration experiment of **1**$[PF_6]_2$ results in binding constants (K_a) of 5.28×10^4 M^{-1} and 4.67×10^4 M^{-1} for $H_2PO_4^-$ and $HP_2O_7^{3-}$, respectively, which is in good agreement with the K_a values obtained from UV–vis titration experiments (2.97×10^4 M^{-1} and 2.45×10^4 M^{-1} for $H_2PO_4^-$ and $HP_2O_7^{3-}$, respectively). High selectivity of **1**$[PF_6]_2$ toward these two anions in acetonitrile is further confirmed by PL intensity measurement of **1**$[PF_6]_2$ upon addition of these two anions in the presence of a large excess of other competitive anions. Further, considerable changes in the lifetime (τ) as well as in the decay pattern of **1**$[PF_6]_2$ in the presence of $H_2PO_4^-$/$HP_2O_7^{3-}$ among all tested anions support the selective binding property of **1**$[PF_6]_2$ toward these two anions. Significant downfield shift of the triazole –CH proton of **1**$[PF_6]_2$ with 1 equiv of $H_2PO_4^-$ ($\Delta\delta$ = 0.26 ppm) and $HP_2O_7^{3-}$ ($\Delta\delta$ = 0.23 ppm) in deuterated dimethyl sulfoxide proclaim binding mechanism via C–H···anion interaction in solution state. Finally, single-crystal X-ray structural analysis confirms the first example of dihydrogen pyrophosphate ($H_2P_2O_7^{2-}$) recognition via solitary C–H···anion interactions.

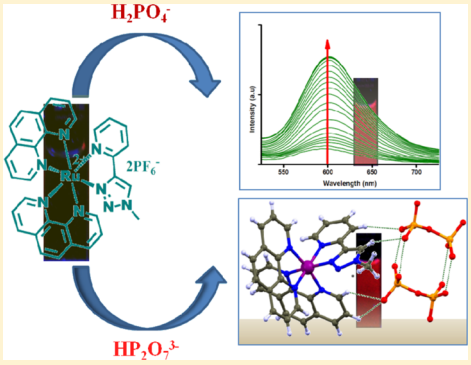

INTRODUCTION

Inorganic phosphates are indispensable for their crucial roles in signal transduction,[1,2] energy storage to living organisms, as well as eutrophication of water body.[3,4] Detection of larger and higher charge analogues of dihydrogen phosphate, that is, pyrophosphate, has attracted growing attention in recent times because of the role played by analogues in real time DNA sequencing and DNA replication catalyzed by DNA polymerase.[5] Receptors consisting of N–H bond donor groups (e.g., indole, pyrrole, ammonium, guanidinium) or cationic C–H bond donor groups (e.g., imidazolium and triazolium)[6] are found to be suitable candidates for such detection. Several reports show participation of 1,2,3-triazole unit in noncovalent interactions.[7] Electronegativity of three nitrogen atoms of the triazole ring polarize the triazole C–H bond, and the lone pair of nitrogen atoms exert a large dipole toward triazole C–H bond. These two effects assist triazole C–H to behave as an amide bond alternative for the recognition of anions.[8] On the other hand, triazole nitrogen centers act as an excellent metal ion coordinating site.[9] Thus, binding of this triazole pyridine unit with a metal center could further enhance the binding ability of the triazole C–H toward anions. However, attachment of a suitable signaling unit is necessary to establish the anion binding event via signaling output.[10] On the other hand, Ru(II) polypyridyl complexes exhibit interesting photophysical/photochemical properties that make them useful as luminescent sensors, dye-sensitized solar cells, photoactive devices, etc.[11] Ru(II) polypyridyl complexes have received a great deal of attention as luminescent sensors because of their interesting photophysical properties such as visible light excitation, large Stokes shift, relatively long excited state lifetime, etc.[12] So, complexation of triazole pyridine unit with Ru(II) center may serve a dual purpose of making triazole C–H a more efficient hydrogen bond donor as well as in establishing anion recognition event via signaling output. Herein, we report a bis-heteroleptic Ru(II) complex of triazole pyridine and phenanthroline hybrid for the selective sensing of $H_2PO_4^-$ and $HP_2O_7^{3-}$ in acetonitrile via C–H···anion interactions. Moreover, single-crystal X-ray analysis reveals the solid-state structural evidence of binding of dihydrogen pyrophosphate with **1**$[PF_6]_2$ by only C–H···anion interactions. To the best of our knowledge, this is the first example of $H_2P_2O_7^{2-}$ recognition via solitary neutral C–H···anion interactions.

RESULTS AND DISCUSSION

Designing Aspect of Complex 1. Recognition of anion generally occurs via interaction of guest anion with the acidic hydrogen of receptor. When the receptor unit is attached with a

Received: May 6, 2014
Published: July 23, 2014

   dx.doi.org/10.1021/ic5010598 | Inorg. Chem. 2014, 53, 8061–8070

Scheme 1. Synthesis of $1[PF_6]_2$

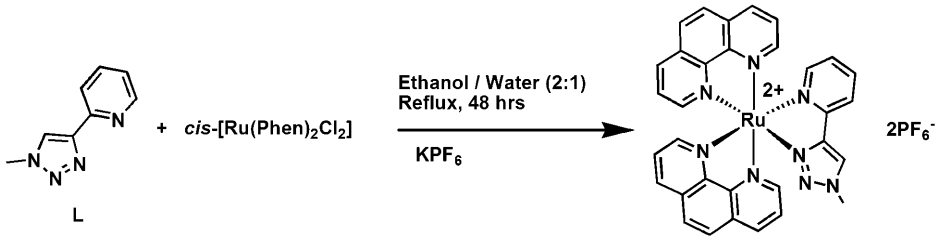

suitable signaling device, the recognition event can be monitored by signaling output. Thus, a suitable signaling unit needs to be integrated with the anion recognition motif. Considering these aspects, we designed the chelating triazole pyridine (**L**) and phenanthroline-based Ru(II) complex ($\mathbf{1}[PF_6]_2$). Thus, the ruthenium(II) center of ($\mathbf{1}[PF_6]_2$) could enhance the acidity of the triazole C−H, which eventually makes C−H a more efficient hydrogen bond donor toward anion. Simultaneously, ruthenium(II) center can also act as a probe to monitor the anion binding event through the change in photophysical properties.

Chemical structure of complex $1(PF_6)_2$

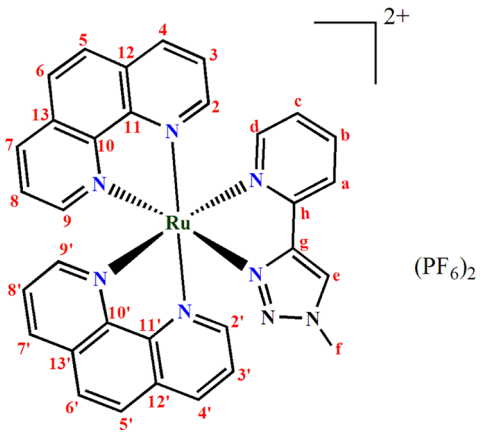

Synthesis and Characterization. The ligand (**L**) and *cis*-$[Ru(Phen)_2Cl_2]$ are synthesized according to the reported literature procedures.[13] Ruthenium(II) complex ($\mathbf{1}[PF_6]_2$) is prepared by refluxing **L** with *cis*-$[Ru(Phen)_2Cl_2]$ in ethanol/water (2:1,v/v) mixture under argon atmosphere for 48 h followed by counteranion exchange of Cl^- with PF_6^- (Scheme 1). The $\mathbf{1}[PF_6]_2$ is characterized by one-dimensional (1D) (^{1}H, DEPT-135, ^{13}C) and two-dimensional (2D) (^{1}H−^{1}H COSY, ^{1}H-DEPT-135 HSQC, and ^{1}H−^{13}C HMBC) NMR, electrospray ionization mass spectrometry (ESI-MS), and elemental analysis techniques. Photophysical properties of $\mathbf{1}[PF_6]_2$ are determined by UV−vis, photoluminescence (PL), and time-resolved spectroscopic methods. 1D and 2D NMR spectra for $\mathbf{1}[PF_6]_2$ in acetone-d_6 (in 500 MHz) at room temperature have shown all expected resonances of phenanthroline and pyridine units. All characteristic peaks in ^{1}H NMR spectrum are assigned by ^{1}H−^{1}H COSY NMR (Figure S2, Supporting Information). All the carbon signals in DEPT-135 (Figure S3, Supporting Information) and ^{13}C NMR (Figure S4, Supporting Information) of $\mathbf{1}[PF_6]_2$ are assigned using HSQC and HMBC (Figures S5 and S6, Supporting Information) NMR spectra.

In ESI-MS two characteristic peaks are found at m/z 311.04 (calcd. 311.06) and 767.08 (calcd. 767.08), which can be assigned as doubly charged ($[C_{32}H_{24}N_8Ru]^{2+}$) and singly charged ($[C_{32}H_{24}N_8Ru(PF_6)]^+$) species, respectively (Figure S7, Supporting Information). The experimental isotopic distribution patterns of the singly- and doubly charged species are matched perfectly with their calculated patterns (Figure S8, Supporting Information).

Photophysical Properties of $1[PF_6]_2$. Photophysical properties of $\mathbf{1}[PF_6]_2$ are determined by UV−vis, PL, and time-resolved spectroscopic methods. The UV−vis spectrum of $\mathbf{1}[PF_6]_2$ shows bands at ~262 (ε = 64 850 M^{-1} cm^{-1}), ~403 (ε = 10 850 M^{-1} cm^{-1}) and ~445 nm (ε = 8637 M^{-1} cm^{-1}) in acetonitrile at 25 °C (Figure S9a, Supporting Information). The band at ~262 nm can be assigned as intraligand (IL) $\pi-\pi^*$ transitions, whereas the bands ~403 nm and ~445 nm could be due to metal-to-ligand charge transfer (MLCT); one from Ru center to phenanthroline unit and another from Ru center to pyridine−triazole unit.[13a] Excitation of $\mathbf{1}[PF_6]_2$ at 403 nm results in broad centered weak luminescence spectrum ~590 nm at room temperature in acetonitrile (Figure S9b, Supporting Information). However, excitation at 445 nm does not perturb the nature of luminescence spectrum achieved in case of excitation at 403 nm, which indicates that the emission is occurring from the same MLCT excited state. $\mathbf{1}[PF_6]_2$ shows rapid decay pattern in acetonitrile with a lifetime ~5 ns as evident from the time-resolved spectroscopic study. This could be due to molecular movement that favors luminescence decay via rotational and vibrational pathways.

Detection of Anions by UV−vis and PL Spectroscopic Methods. $\mathbf{1}[PF_6]_2$ is explored for the recognition and sensing of various anions like halides, nitrate, acetate, benzoate, hydrogen carbonate, hydroxide, hydrogensulfate, phosphates, and perchlorate as their corresponding tetrabutylammonium salts by UV−vis and PL studies. Upon addition of various anions to the acetonitrile solution of $\mathbf{1}[PF_6]_2$ (40 μM), MLCT band at 445 nm is red-shifted only in the presence of $H_2PO_4^-$ and $HP_2O_7^{3-}$ (1 equiv), whereas addition of 10 equiv of other anions do not make any change in the UV−vis spectrum of $\mathbf{1}[PF_6]_2$ (Figure 1a). This selective binding of $H_2PO_4^-$ and $HP_2O_7^{3-}$ over other anions makes $\mathbf{1}[PF_6]_2$ a selective chemosensor for $H_2PO_4^-$ and $HP_2O_7^{3-}$.

Selective sensing of $\mathbf{1}[PF_6]_2$ toward $H_2PO_4^-$ and $HP_2O_7^{3-}$ is further established by PL studies. Broad centered luminescence spectrum of $\mathbf{1}[PF_6]_2$ remained unperturbed upon addition of different anions except $H_2PO_4^-$ and $HP_2O_7^{3-}$. Addition of 10 equiv of $H_2PO_4^-$ and $HP_2O_7^{3-}$ enhances the emission by 6-fold and 3-fold, respectively, with a 10 nm red shift (Figure 1b). It can be assumed that the binding of $H_2PO_4^-$ and $HP_2O_7^{3-}$ with weakly luminescent $\mathbf{1}[PF_6]_2$ causes rigidity of the framework and lowers the nonradiative decay via rotational and vibrational relaxation pathways, thus enhancing its emission intensity.[14] This selective emission enhancement in the presence of these two anions

dx.doi.org/10.1021/ic5010598 | Inorg. Chem. 2014, 53, 8061−8070

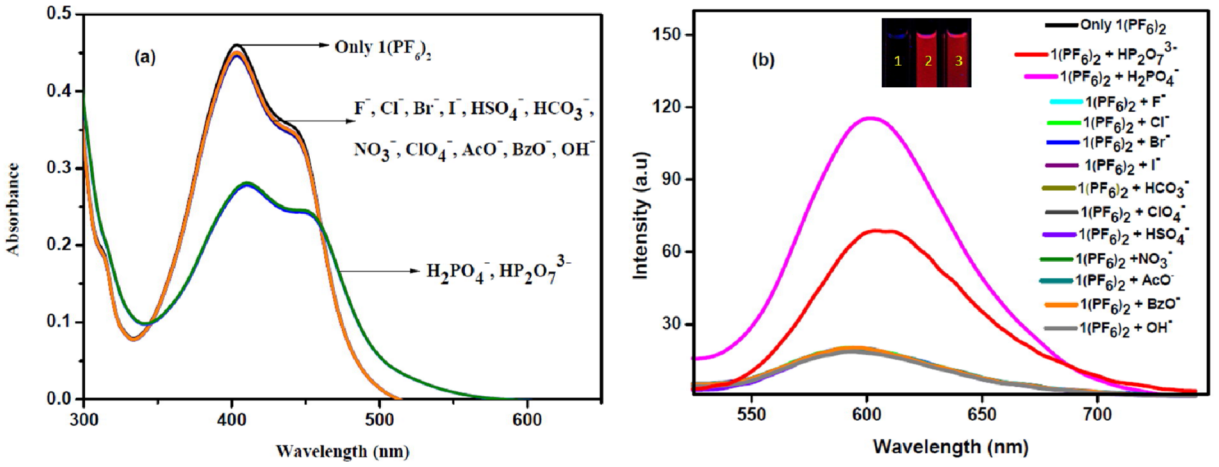

Figure 1. (a) Changes in UV−vis of $\mathbf{1}[PF_6]_2$ (40 μM) in the presence of various anions (10 equiv). (b) PL spectrum of $\mathbf{1}[PF_6]_2$ (10 μM) in the presence of various anions (10 equiv) in acetonitrile at 25 °C; (λ_{ex} = 403 nm, excitation and emission slit width = 5.0 nm). Anions were used as their corresponding tetrabutylammonium salts. (inset) Photograph of (1) $\mathbf{1}[PF_6]_2$, (2) $\mathbf{1}[PF_6]_2$ in the presence of $H_2PO_4^-$, and (3) $\mathbf{1}[PF_6]_2$ in the presence of $HP_2O_7^{3-}$ under UV light irradiation.

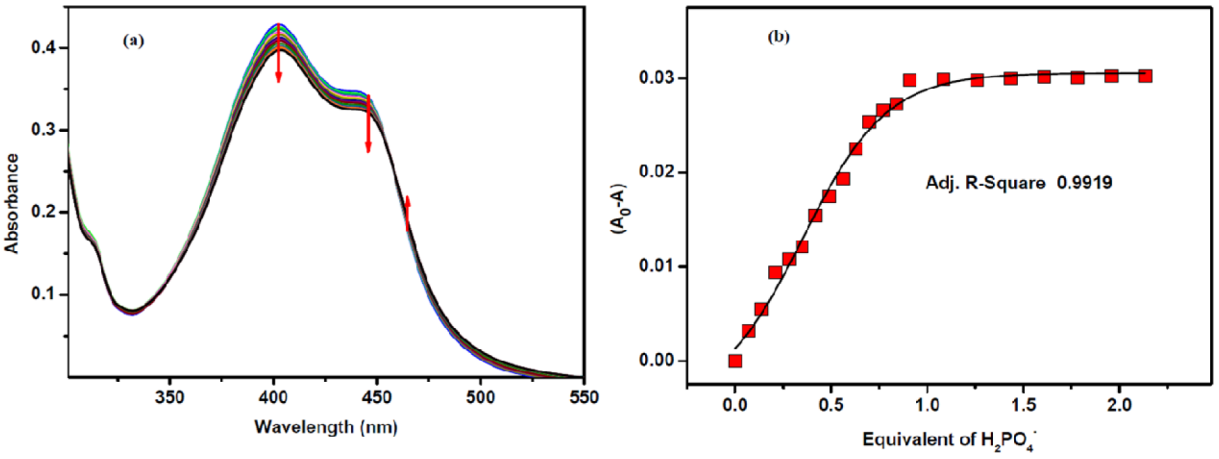

Figure 2. (a) Changes in UV−vis spectrum of $\mathbf{1}[PF_6]_2$ (40 μM) upon the addition of increasing amounts (0−2 equiv) of $TBAH_2PO_4$ in acetonitrile at 25 °C. (b) Plot of changes in absorbance against different equiv (0−2) of $TBAH_2PO_4$ added.

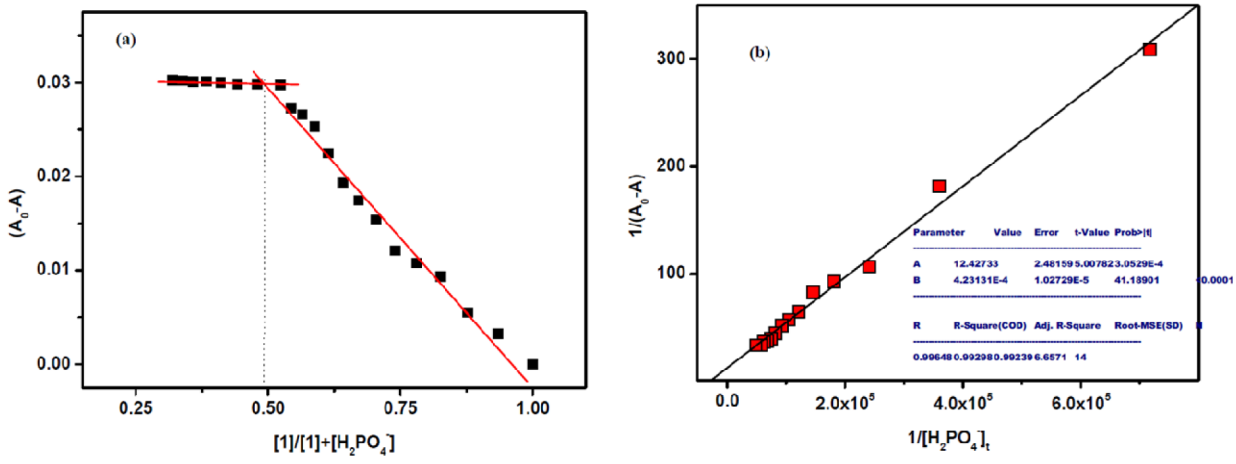

Figure 3. (a) Job's plot and (b) Benesi−Hildebrand plot for $\mathbf{1}[PF_6]_2$ with $H_2PO_4^-$ from UV−vis titration in acetonitrile at 25 °C.

allows us to detect $H_2PO_4^-$ and $HP_2O_7^{3-}$ over other tested anions.

UV−vis and PL spectra of $\mathbf{1}[PF_6]_2$ in acetonitrile remains unperturbed even in the presence of 10 equiv of OH^-. However, with the addition of 1 equiv of $H_2PO_4^-$ to the above solution, the MLCT band of the complex shifts from 445 to 465 nm, and enhancement in the emission intensity is observed with a 10 nm red shift as observed in the absence of OH^-

dx.doi.org/10.1021/ic5010598 | Inorg. Chem. 2014, 53, 8061−8070

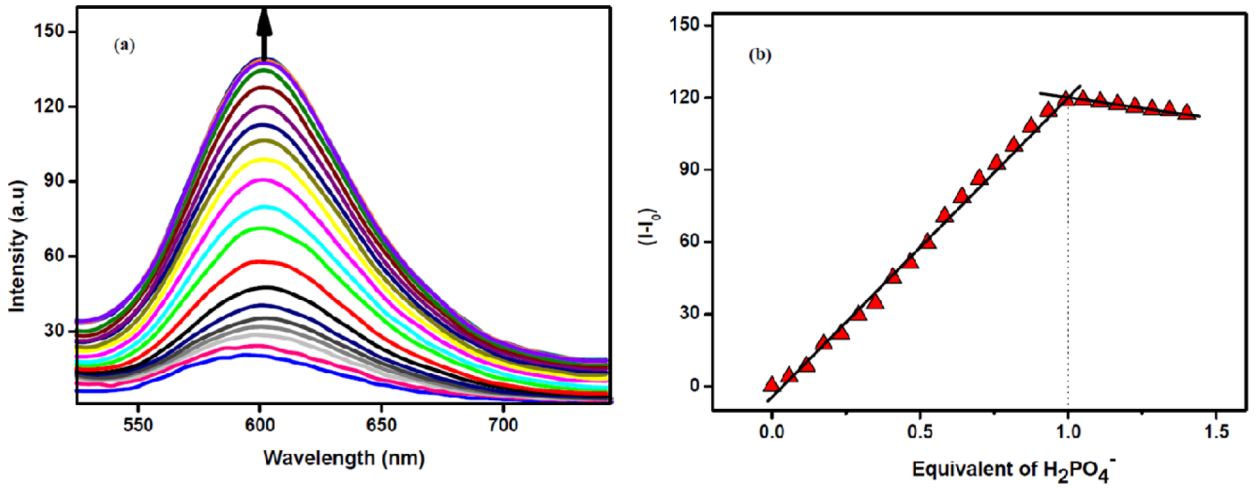

Figure 4. (a) PL titration profile of $\mathbf{1}[PF_6]_2$ (10 μM) upon the addition of increasing amounts (0–1.5 equiv) of $H_2PO_4^-$ in acetonitrile at 25 °C. (b) Changes in emission intensity against different equiv (0–1.5) of $H_2PO_4^-$.

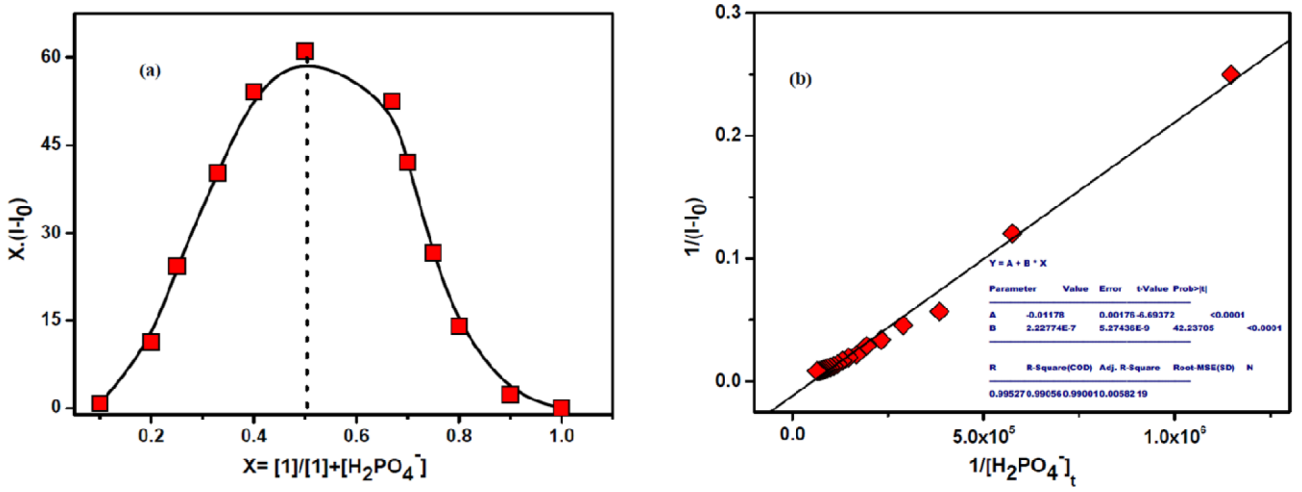

Figure 5. (a) Job plot of PL of $\mathbf{1}[PF_6]_2$ with $H_2PO_4^-$ in acetonitrile at 25 °C ($[\mathbf{1}(PF_6)_2] = [H_2PO_4^-] = 20\ \mu$M). (b) Benesi–Hildebrand plot from PL titration of $\mathbf{1}[PF_6]_2$ with $H_2PO_4^-$ showing good fitting for the 1:1 model.

(Supporting Information, Figure S10). No further change in the UV–vis and PL spectra is observed after further addition of excess $H_2PO_4^-$ (Supporting Information, Figure S10).

UV–vis and PL Titration Experiment. Binding affinity of $\mathbf{1}[PF_6]_2$ toward $H_2PO_4^-$ and $HP_2O_7^{3-}$ is monitored via UV–vis and PL titration experiments of $\mathbf{1}[PF_6]_2$ with these two anions in acetonitrile. Upon increasing the amount of these two anions to the acetonitrile solution of $\mathbf{1}[PF_6]_2$ (40 μM), the absorption peaks at 403 (ε = 10 850 M^{-1} cm^{-1}) and ~445 nm (ε = 8637 M^{-1} cm^{-1}) decrease with concomitant increase in the absorbance peak at ~465 nm (ε = 5751 M^{-1} cm^{-1}). A clear isosbestic point is observed at 455 nm upon 0–1 equiv addition of these two guest anions, which clearly indicates the existence of single equilibrium between $\mathbf{1}[PF_6]_2$ and corresponding **1**-anions adduct (Figure 2a and Figure S11, Supporting Information). No further change is observed upon addition of anionic guest beyond 1 equiv (Figure 2b and Figure S12, Supporting Information), confirming the 1:1 stoichiometric binding pattern between $\mathbf{1}[PF_6]_2$ and the corresponding anions (Figure 3a and Figure S13, Supporting Information). The UV–vis titration data shows best fit for 1:1 model and association constants are calculated as 2.97 × 10^4 M^{-1} and 2.45 × 10^4 M^{-1} for $H_2PO_4^-$ and $HP_2O_7^{3-}$, respectively, from

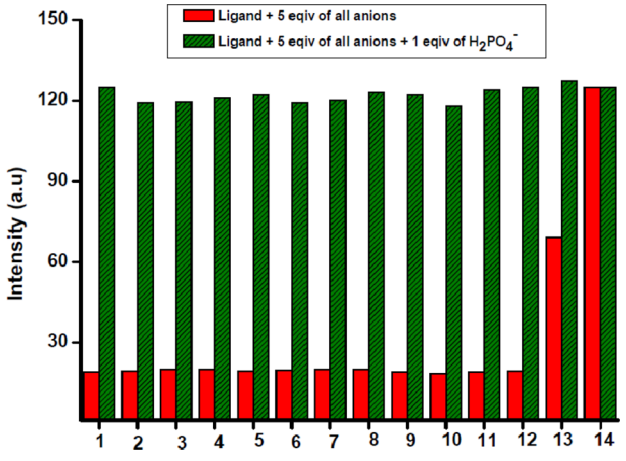

Figure 6. Selectivity studies of $\mathbf{1}[PF_6]_2$ with $H_2PO_4^-$ in the presence of other anions in acetonitrile. Color code: red bars correspond to $\mathbf{1}[PF_6]_2$ in the presence of all anions, and green bars correspond to $\mathbf{1}[PF_6]_2$ in the presence of other competitive anions and $H_2PO_4^-$. Number code: (1) $\mathbf{1}[PF_6]_2$ (2) F^- (3) Cl^- (4) Br^- (5) I^- (6) AcO^- (7) BzO^- (8) NO_3^- (9) HCO_3^- (10) HO^- (11) ClO_4^- (12) HSO_4^- (13) $HP_2O_7^{3-}$ (14) $H_2PO_4^-$.

dx.doi.org/10.1021/ic5010598 | Inorg. Chem. 2014, 53, 8061–8070

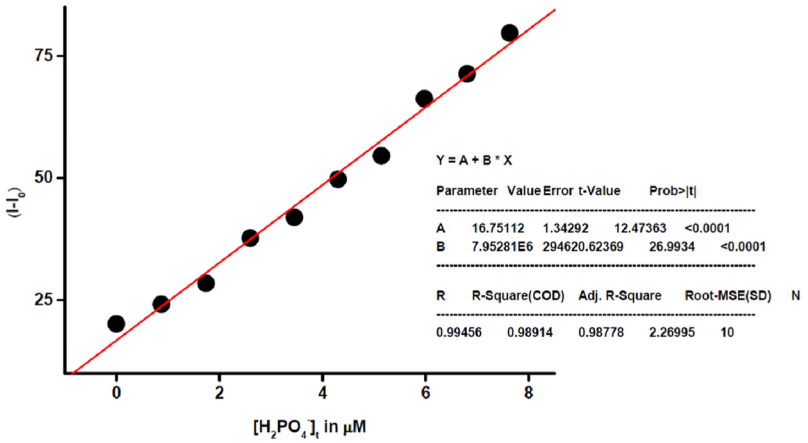

Figure 7. A calibration curve for $H_2PO_4^-$ over the concentration range between 0 and 10.0 μM derived from the PL titration with probe $\mathbf{1}[PF_6]_2$ (10.0 μM).

Table 1. List of Lifetimes of $\mathbf{1}[PF_6]_2$ in the Presence of Various Anions in Acetonitrile

entry	lifetime (ns)
$\mathbf{1}[PF_6]_2$	5.45
$\mathbf{1}[PF_6]_2 + F^-$	5.44
$\mathbf{1}[PF_6]_2 + Cl^-$	4.45
$\mathbf{1}[PF_6]_2 + Br^-$	5.39
$\mathbf{1}[PF_6]_2 + NO_3^-$	4.43
$\mathbf{1}[PF_6]_2 + AcO^-$	4.61
$\mathbf{1}[PF_6]_2 + BzO^-$	4.38
$\mathbf{1}[PF_6]_2 + HCO_3^-$	4.27
$\mathbf{1}[PF_6]_2 + ClO_4^-$	5.29
$\mathbf{1}[PF_6]_2 + HSO_4^-$	5.39
$\mathbf{1}[PF_6]_2 + HP_2O_7^{3-}$	12.01
$\mathbf{1}[PF_6]_2 + H_2PO_4^-$	28.60

Benesi–Hildebrand plot analysis (Figure 3b and Figure S14, Supporting Information).

PL titration experiment is also carried out by gradual addition of guest anion to the acetonitrile solution of $\mathbf{1}[PF_6]_2$ (10 μM). Upon addition of increasing amount of guest anions ($H_2PO_4^-$ and $HP_2O_7^{3-}$), gradual increases in PL intensity (Figure 4a and Figure S15, Supporting Information) at 600 nm are observed up to 1 equiv addition of guest anions (Figure 4b and Figure S16, Supporting Information). The Job plot analysis shows the inflection point at 0.5 indicating the 1:1 stoichiometry between the host and guest (Figure 5a and S17, Supporting Information). Binding constants are calculated as 5.28×10^4 M^{-1} and 4.67×10^4 M^{-1} for $H_2PO_4^-$ and $HP_2O_7^{3-}$, respectively, from Benesi–Hildebrand plot analysis (Figure 5b and Figure S18, Supporting Information).

When the PL intensity change $(I - I_0)$ of $\mathbf{1}[PF_6]_2$ is plotted against different concentrations of $H_2PO_4^-$ and $HP_2O_7^{3-}$ a good linear relationship is shown from 0 to 15 mM concentration of these two anions, and after that no further change is observed. This linear relationship between $(I - I_0)$ and concentration of corresponding anion also helps to determine the concentration of these anions in unknown samples (Figure S19, Supporting Information).

Selectivity and Sensitivity. To prove the selectivity of $\mathbf{1}[PF_6]_2$ toward $H_2PO_4^-$ and $HP_2O_7^{3-}$ over other anions, competitive PL study is carried out. From the anion detection experiment in PL channels, no change in luminescence spectrum of $\mathbf{1}[PF_6]_2$ is observed in the presence of other competitive anions

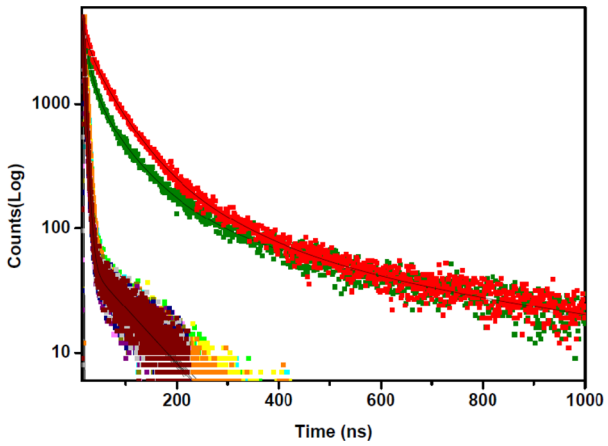

Figure 8. Changes in the time-resolved luminescence decays of $\mathbf{1}[PF_6]_2$ (10.0 μM) in acetonitrile solution at 25 °C upon addition of different anions as their corresponding tetrabutylammonium salts. Color code: red spectrum corresponds to $\mathbf{1} + H_2PO_4^-$, green spectrum corresponds to $\mathbf{1} + HP_2O_7^{3-}$.

(e.g., F^-, Cl^-, Br^-, I^-, HCO_3^-, NO_3^-, ClO_4^-, AcO^-, BzO^-, HO^-, HSO_4^-) except for $H_2PO_4^-$ and $HP_2O_7^{3-}$. However, $\mathbf{1}[PF_6]_2$ shows enhancement of emission upon addition of $H_2PO_4^-$ and $HP_2O_7^{3-}$ (1 equiv) even in the presence of a large excess (5 equiv) of other competitive anions (Figure 6). This selective emission enhancement with these two anions, even in the presence of other competitive anions, establishes this complex as a useful candidate for the selective detection of these anions in acetonitrile.

This selective detection of $H_2PO_4^-$ and $HP_2O_7^{3-}$ over other competitive anions via emission enhancement could allow determining the detection limit for these two anions in acetonitrile. The PL intensity change of $\mathbf{1}[PF_6]_2$ $(I - I_0)$ plotted against varying concentrations of $H_2PO_4^-$ and $HP_2O_7^{3-}$ shows a good linear relationship (Figure 7 and Figure S20, Supporting Information), and the detection limit (DL) is calculated from the equation DL = 3 × SD/slope,[15] where SD corresponds to standard deviation of blank sample obtained by 10 consecutive scans of the blank sample. Limit of detection is found as low as ca. 0.25 μ(M) and 0.45 μ(M) for $H_2PO_4^-$ and $HP_2O_7^{3-}$, respectively.

Time-Resolved Spectroscopic Study. Lifetime-based detection is advantageous over simple luminescence intensity-based detections.[16] Ruthenium polypyridyl complexes are

dx.doi.org/10.1021/ic5010598 | Inorg. Chem. 2014, 53, 8061–8070

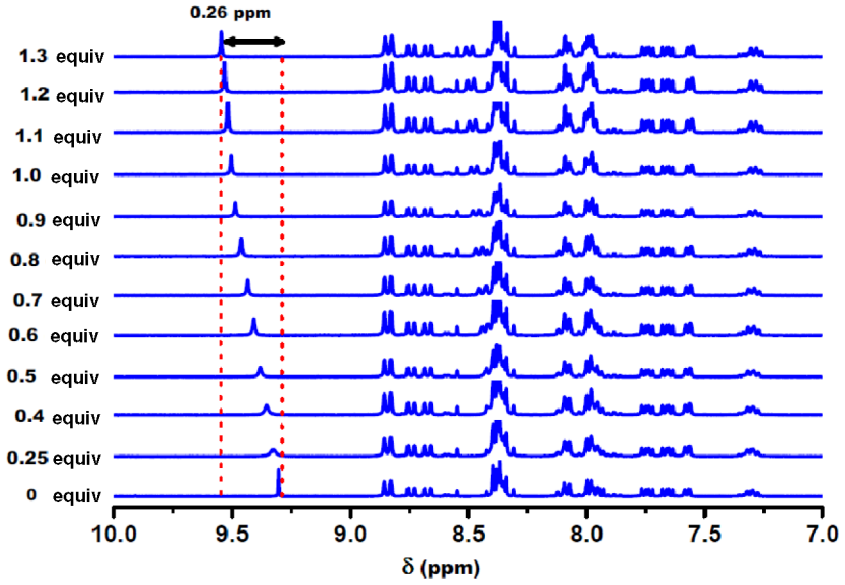

Figure 9. Changes in ^{1}H NMR of $\mathbf{1}[PF_6]_2$ upon addition of increasing amounts of $H_2PO_4^-$ in DMSO-d_6 solvent.

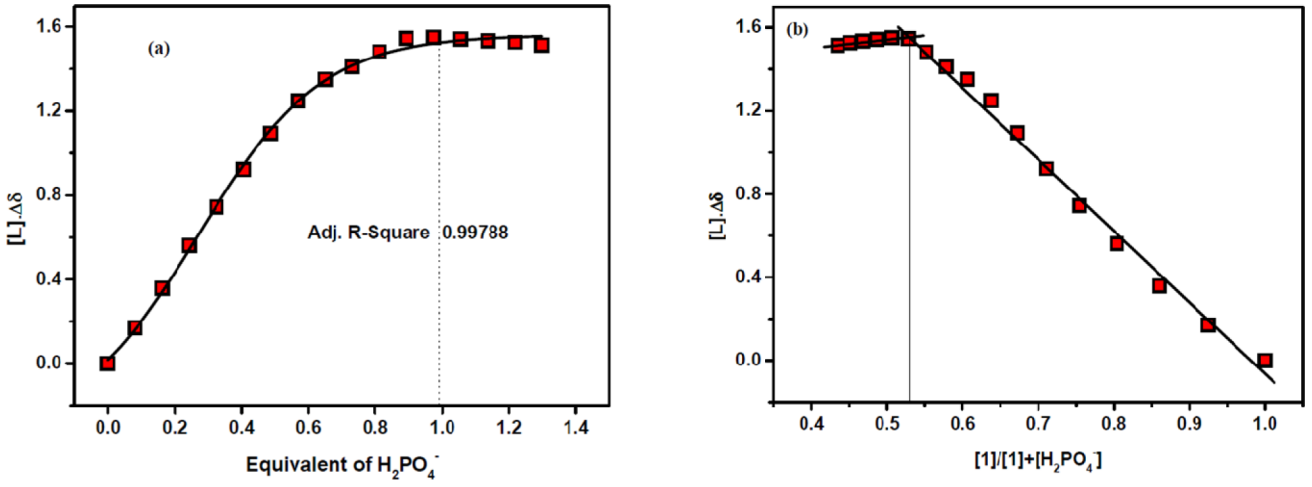

Figure 10. (a) Job's plot from ^{1}H NMR titration of $\mathbf{1}[PF_6]_2$ with $H_2PO_4^-$. (b) Changes in chemical shift upon the addition of various equivalents of $H_2PO_4^-$ to the solution of $\mathbf{1}[PF_6]_2$ in DMSO-d_6 at 25 °C.

important from the aspect of bearing relatively larger luminescence lifetimes than their purely organic counter parts. Keeping this in mind, lifetime measurements of free receptor ($\mathbf{1}[PF_6]_2$) and receptor in the presence of various anions are carried out in acetonitrile at room temperature. Lifetimes calculated for free receptor ($\mathbf{1}[PF_6]_2$) and receptor in the presence of all competitive anions (F^-, Cl^-, Br^-, NO_3^-, AcO^-, BzO^-, ClO_4^-, HCO_3^-, HSO_4^-) result in the same value of ~5 ns (Table 1) except for $H_2PO_4^-$ (29 ns) and $HP_2O_7^{3-}$ (12 ns). The decay profile also shows a similar decay pattern for $\mathbf{1}[PF_6]_2$ as well as in the presence of all anions except $H_2PO_4^-$ and $HP_2O_7^{3-}$ (Figure 8). Different decay patterns obtained for $H_2PO_4^-$ and $HP_2O_7^{3-}$ can be fitted as a sum of two exponentials. This biexponential decay pattern obtained in case of these two anions indicate the existence of two different species in solution; one of them may be the free receptor ($\mathbf{1}[PF_6]_2$) with shorter lifetime, and the other is assigned to the hydrogen-bonded adduct of the receptor with anion involving relatively longer lifetimes. In the presence of these two anions, the hydrogen-bonded adduct contributes more to the lifetime; as a result, the overall lifetime of the receptor ($\mathbf{1}[PF_6]_2$) is enhanced in the presence of these two anions (12 and 28.6 ns for $H_2PO_4^-$ and $HP_2O_7^{3-}$, respectively). This selective lifetime enhancement in the presence of these two anions ($H_2PO_4^-$ and $HP_2O_7^{3-}$) allows us to ascertain this metalloreceptor a suitable lifetime-based sensor for these two anions.

^{1}H NMR Titration Experiment. To gain insight into the mode of interaction between $\mathbf{1}[PF_6]_2$ and $H_2PO_4^-/HP_2O_7^{3-}$, ^{1}H NMR titration experiment is carried out in deuterated dimethyl sulfoxide (DMSO-d_6). Upon addition of increasing amounts of various anions the acidic triazole proton (H_e of $\mathbf{1}[PF_6]_2$) shows a gradual downfield shift only in the presence of 1 equiv of $H_2PO_4^-$ and $HP_2O_7^{3-}$ (Figure 9, 10a and Figure S21, S22a Supporting Information). The addition of 1 equiv of other competitive anions (i.e., F^-, Cl^-, AcO^-, NO_3^-, HSO_4^-, etc.) does not induce any noticeable change in the ^{1}H NMR spectrum of $\mathbf{1}[PF_6]_2$. However, addition of higher equiv (3 equiv or more) of the highly basic anions, that is, F^- and AcO^-, shows downfield shifts ($\Delta\delta$ = 0.15 ppm) of the triazole proton, indicating interaction of these two basic anions with the acidic triazole proton at high analyte concentration (Figure S23, Supporting Information).

dx.doi.org/10.1021/ic5010598 | Inorg. Chem. 2014, 53, 8061−8070

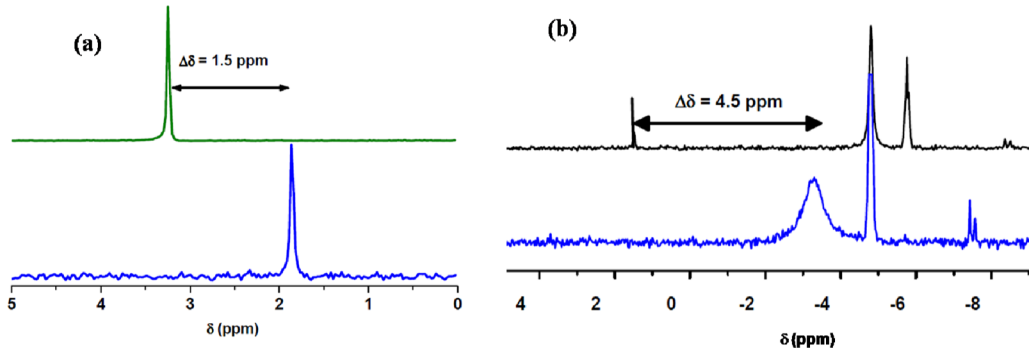

Figure 11. (a) ^{31}P NMR of $TBAH_2PO_4$ (bottom blue spectra) and in the presence of 1 equiv of $\mathbf{1}[PF_6]_2$ (top green spectra). (b) ^{31}P NMR of $TBA_3HP_2O_7$ (bottom blue spectra) and in the presence of 1 equiv of $\mathbf{1}[PF_6]_2$ (top black spectra) in DMSO-d_6, PPh_3 as an external standard (−4.8 ppm in DMSO-d_6).

During the ^{1}H NMR titration of $\mathbf{1}[PF_6]_2$ with 0−1 equiv of $H_2PO_4^-$ the sharp singlet at 9.30 ppm (corresponding to the triazole proton of $\mathbf{1}[PF_6]_2$) shows downfield shift to 9.56 ppm (0.26 ppm shift), whereas in case of $HP_2O_7^{3-}$ this shift is 0.23 ppm (from 9.30 to 9.53 ppm). However, this downfield shift of triazole proton in the presence of $H_2PO_4^-/HP_2O_7^{3-}$ suggests that phosphate binding occurs through the involvement of this triazole C−H proton. The Job's plot analysis from ^{1}H NMR titration data shows 1:1 host/guest stoichiometric binding between **1** and these two anions (Figure 10b and Figure S22b, Supporting Information). From ^{1}H NMR titration experiments log k values are calculated as 4.75 and 3.54 for $HP_2O_7^{3-}$ and $H_2PO_4^-$, respectively.

^{31}P NMR Experiment. ^{31}P NMR of free $H_2PO_4^-/HP_2O_7^{3-}$ as well as in the presence of 1 equiv of $\mathbf{1}[PF_6]_2$ are recorded in DMSO-d_6 using triphenylphosphine (PPh_3) as an external standard (−4.8 ppm in DMSO-d_6). This ^{31}P NMR spectrum shows significant downfield shift of free anion signal upon addition of $\mathbf{1}[PF_6]_2$. Initial ^{31}P signal of free $H_2PO_4^-$ at 1.85 ppm is shifted to 3.24 ppm (Figure 11a), whereas in the case of $HP_2O_7^{3-}$ initial ^{31}P signals at −3.31 and −7.44 ppm are shifted to 1.48 and −5.77 ppm, respectively (Figure 11b). This downfield shift of ^{31}P signals of free $H_2PO_4^-$ and $HP_2O_7^{3-}$ upon addition of equivalent amounts of $\mathbf{1}[PF_6]_2$ indicates that the binding of these two anions must be occurring through the participation of neighboring oxygen centers of P atoms.

Single-Crystal X-ray Diffraction Study. Pyrophosphate adduct of **1**, namely, ($\mathbf{1}[H_2P_2O_7]$), is crystallized by slow evaporation of **1** with tris-tetrabutylammonium hydrogenpyrophosphate from DMSO solvent. $\mathbf{1}[H_2P_2O_7]$ crystallizes in triclinic crystal system with $P\bar{1}$ space group. Detailed crystallographic parameters of $\mathbf{1}[H_2P_2O_7]$ are listed in Table 1S, Supporting Information. Asymmetric unit of $\mathbf{1}[H_2P_2O_7]$ contains complex **1**, one disordered dihydrogenpyrophosphate ($H_2P_2O_7^{2-}$), and one disordered DMSO solvent. Structural analysis reveals that Ru(II) center adopts octahedral geometry through tris-bidentate coordination of two ancillary phenanthrolines and one chelating triazole pyridine unit (Figure 12). The Ru−N bond distances in $\mathbf{1}[H_2P_2O_7]$ are in the range of 2.044−2.089 Å, while trans N−Ru−N angles are in the range of 170.46−174.46° (Table 2S, Supporting Information), which matches well with previously reported ruthenium polypyridyl complexes.[17] Interestingly, $H_2P_2O_7^{2-}$ binding in $\mathbf{1}[H_2P_2O_7]$ is assisted by multiple C−H···O interactions between O atoms of $H_2P_2O_7^{2-}$ and acidic C−H protons of **1**. In $\mathbf{1}[H_2P_2O_7]$, C−O distances vary from 3.145 to3.533 Å, whereas C−H···O angles vary from 121.24° to 169.44°. Hydrogen

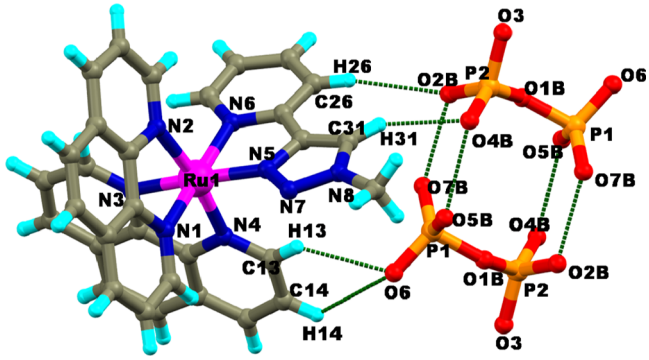

Figure 12. Single-crystal X-ray diffraction structure of $\mathbf{1}[H_2P_2O_7]$. Solvent molecule has been omitted for clarity.

Table 2. List of Hydrogen Bonding Parameters in $\mathbf{1}[H_2P_2O_7]$

D−H···O	H···O (Å)	C···O (Å)	∠D−H···O (deg)
C31−H31···O4B	2.351	3.176	147.66
C26−H26···O2B	2.626	3.533	165.34
C12−H12···O6	2.278	3.197	169.44
C13−H13···O6	2.607	3.190	121.24
C14−H14···O6	2.531	3.145	123.87

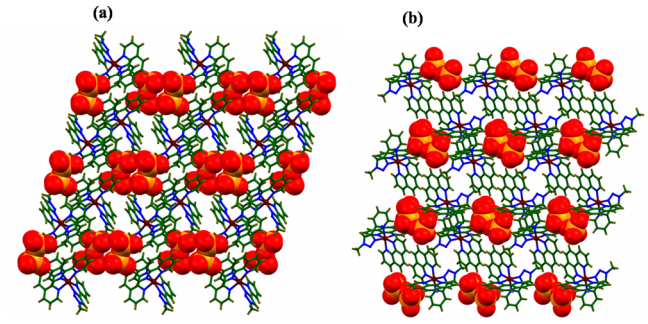

Figure 13. A slice of hydrogen-bonded adduct obtained by assembly of $\mathbf{1}[H_2P_2O_7]$ along crystallographic (a) b axis and (b) c axis.

bonding parameters in $\mathbf{1}[H_2P_2O_7]$ are listed in Table 2. Analysis of crystal packing in $\mathbf{1}[H_2P_2O_7]$ reveals that the complex forms three-dimensional (3D) network via C−H···O interactions between O atoms of $H_2P_2O_7^{2-}$ and acidic C−H protons of **1** (Figure 13). In this context, it is noteworthy to mention that Sessler et al. have first reported structural evidence of pyrophosphate encapsulation by a pyrrolyl-based triazolophane receptor.[6a] To the best of our knowledge, $\mathbf{1}[H_2P_2O_7]$ shows the first solid-state structural

dx.doi.org/10.1021/ic5010598 | Inorg. Chem. 2014, 53, 8061−8070

evidence of $H_2P_2O_7^{2-}$ binding via solely C−H···anion interactions. Crystals of **1**$[H_2P_2O_7]$ are characterized by ^{1}H NMR (Figure S24, Supporting Information), UV−vis, and PL (Figure S25, Supporting Information) spectroscopic techniques.

CONCLUSIONS

In conclusion, we synthesized a simple bis-heteroleptic ruthenium(II) complex of a click-derived triazole-pyridine unit as a selective molecular probe toward detection of dihydrogen phosphate ($H_2PO_4^-$) and hydrogen pyrophosphate ($HP_2O_7^{3-}$). The receptor functions as a luminescence OFF-ON sensor for $H_2PO_4^-$/$HP_2O_7^{3-}$. The ^{1}H NMR titration experiment elucidated the mode of binding of anions via C−H···anion interactions. The calculated detection limit suggests that the complex can selectively detect and quantify these two anions ($H_2PO_4^-$ and $HP_2O_7^{3-}$) at submicromolar level even in the presence of other competitive anions. Further, structural analysis confirms binding of $H_2P_2O_7^{2-}$ via the participation of C−H···anion interactions. The present work serves to highlight the utility of anion binding motif consisting only C−H functionality toward decoration of new generation anion sensors.

EXPERIMENTAL SECTION

Materials. All reactions were carried out in argon gas atmosphere followed by workup at ambient conditions. Acetonitrile was dried over CaH_2 and was collected before use. $RuCl_3{\cdot}xH_2O$, deuterated solvents, tetrabutylammonium salts of F^-, Cl^-, Br^-, I^-, AcO^-, BzO^-, ClO_4^-, NO_3^-, HCO_3^-, HO^-, HSO_4^-, $H_2PO_4^-$, and $HP_2O_7^{3-}$ were purchased from Sigma-Aldrich and were used as received. Ethanol was purchased from Spectrochem Pvt. Ltd., India. Millipore water was used for the synthesis of **1**$[PF_6]_2$. Ethanol was distilled and degassed prior to the synthesis of **1**$[PF_6]_2$.

Methods. Fourier transform infrared (FTIR) spectra were recorded on SHIMADZU FTIR-8400S IR spectrophotometer with KBr pellets. High-resolution mass spectrometry (HRMS) analysis was performed on QToF−Micro YA 263 Mass spectrometer in positive ESI mode. ^{1}H, ^{13}C, DEPT, COSY, HSQC, and HMBC-NMR experiments were carried out on FT-NMR Bruker DPX 500 MHz NMR spectrometer. The absorption and emission studies were performed in a PerkinElmer Lambda 900 UV−vis−NIR spectrometer (NIR = near-infrared) (with a quartz cuvette of path length 1 cm) and PerkinElmer LS-55 spectrofluorimeter, respectively. Elemental analysis was performed on PerkinElmer 2500 series II elemental analyzer, PerkinElmer, USA. For the time-correlated single-photon counting (TCSPC) measurements, samples were excited at 405 nm using picoseconds diode laser (IBH Nanoled-07) in an IBH Fluorocube apparatus. The luminescence decay data were recorded on a Hamamatsu MCP photomultiplier (R3809) and were analyzed using IBH DAS6 software. Chemical shifts for ^{1}H and ^{13}C NMR were reported in parts per million (ppm), calibrated to the residual solvent peak set, with coupling constants reported in Hertz (Hz). ^{1}H NMR titration was carried out on 300/400 MHz Bruker DPX NMR spectrometer.

Calculation of Association Constants. Associations between **1**$[PF_6]_2$ and $H_2PO_4^-$/$HP_2O_7^{3-}$ were calculated using UV and PL titration data. Association constants were calculated using Benesi−Hildebrand equation.[1]

$$1/(I - I_0) = 1/(I - I_s) + 1/\{k(I - I_0)[\text{guest}]\} \quad (1)$$

I_0 is the PL intensity of free **1**$[PF_6]_2$, I is the PL intensity upon each addition of guest anion. I_s is the PL intensity at saturation point. The errors were calculated within 10%.

Calculation of Excited-State Lifetimes. Experimental time-resolved luminescence decays were analyzed using the following equation:[2]

$$P(t) = b + \sum \alpha_i \exp(-t/\tau_i) \quad (2)$$

Here, $P(t)$ is the decay, n is the number of discrete emissive species, b is a baseline correction, α_i is the pre-exponential factor, and τ_i is the excited-state luminescence lifetimes associated with the i^{th} component, respectively. In case of multiexponential decays the average lifetime $\langle\tau\rangle$ was calculated from the following equation:[3]

$$\langle\tau\rangle = \sum a_i\tau_i \quad (3)$$

where a_i is contribution of the i^{th} decay component and

$$a_i = \alpha_i/\sum \alpha_i \quad (4)$$

X-ray Crystallographic Refinement Details. The crystallographic details of complex **1**$[H_2P_2O_7]$ are given in Table S2, Supporting Information. A crystal of suitable size was collected from the mother liquor, dipped in paratone oil, and was mounted on the tip of a glass fiber. Epoxy resin was used to cement the crystal on the top of the glass fiber. Intensity data of the crystal was collected using Mo Kα (λ = 0.7107 Å) radiation on a Bruker SMART APEX diffractometer, which was equipped with a CCD area detector at 150 K. SAINT[18a] software was used to process the data integration and reduction. SADABS[18b] was used to apply an empirical absorption correction to the collected reflections. Direct method was used to solve the structure using SHELXTL[19] and was refined on F^2 by the full-matrix least-squares technique using the SHELXL-97[20] program package. PLATON-97[21] and MERCURY 3.1[22] were used to generate graphics. The non-hydrogen atoms were refined anisotropically until convergence. Hydrogen atoms were geometrically fixed at idealized positions in the case of **1**$[H_2P_2O_7]$. Even though the data were collected at 150 K several times, we are unable to assign electron density for some solvent molecules in the unit cell. The routine SQUEEZE[22] was applied to intensity data of **1**$[H_2P_2O_7]$ to take into account the disordered solvent molecules. The O1, O2, and O4 atoms of dihydrogenpyrophosphate ($H_2P_2O_7^{2-}$) anion in **1**$[H_2P_2O_7]$ are disordered over three positions.

Synthesis. *Synthesis of [2-(1-Methyl-1H-1,2,3-triazol-4-yl)-pyridine] (L).* Ligand **L** was synthesized following the reported literature procedure[13a] and was used for the synthesis of complex **1**.

*Synthesis of [Bis(1,10-phenanthroline)(pytl-Me)]ruthenium(II) dihexafluorophosphate] (**1**$[PF_6]_2$).* *cis*-$[Ru(Phen)_2Cl_2]$ was synthesized following the reported literature procedure[13b] and was used for the synthesis of complex **1**. **L** (0.06g, 0.37 mmol) and *cis*-$[Ru(Phen)_2Cl_2]$ (0.195g, 0.37 mmol) were dissolved in 30 mL of well-degassed ethanol−water mixture (2:1 v/v). The mixture was heated to reflux under argon atmosphere for 48 h, when the color of the solution became dark red. Thereafter the reaction mixture was cooled to room temperature, and ethanol was evaporated in the rotary evaporator. Then it was treated with excess of KPF_6 (450 mg). The orange-red precipitate was filtered, washed well with water, and dried under vacuum. This crude product was then purified by Silica gel column chromatography ($CH_3CN/H_2O/KNO_3$ 80:19:1 as eluent). The dark orange-red band was collected as nitrate salt. Volume of the collected portion was reduced by rotary evaporation, and excess of KPF_6 was added to the solution. Orange-red product was precipitated from the mixture, which was filtered and washed well by water. The compound was air-dried finally to get desired product (**1**$[PF_6]_2$) as orange-red crystalline solid (0.226g, 68% yield). Anal. calcd. for $C_{32}H_{24}F_{12}N_8P_2Ru$ (MW = 911.59) C, 42.16; H, 2.65; N, 12.23; found: C, 42.60; H, 2.49; N, 12.78%. FTIR in KBr disc (ν/cm^{-1}): 3437, 1620, 1512, 1456, 1429, 1049, 841, 777, 721. ESI-MS $C_{32}H_{24}N_8Ru$: calcd, m/z = 311.06; found, m/z = 311.04. ESI-MS $C_{32}H_{24}N_8RuPF_6^+$: calcd, m/z = 767.08; found, m/z = 767.08. ^{1}H NMR (500 MHz, acetone-d_6): δ = 9.155 (s, 1H, H_e), 8.880−8.835 (t, 2H, $H_{4,4'}$), 8.768−8.698 (m, 2H, $H_{7,7'}$), 8.657−8.614 (m, 2H, $H_{2,2'}$), 8.428−8.357 (m, 6H, $H_{d,6,6',5,5',9'}$), 8.263 (d, 1H, H_9), 8.122−8.082 (t, 1H, H_b), 8.034−7.958 (m, 2H, $H_{3,3'}$), 7.894−7.880 (d, 1H, H_a), 7.795−7.761 (t, 1H, $H_{8'}$), 7.722−7.689 (t, 1H, H_8), 7.339−7.306 (t, 1H, H_c), 4.141 (s, 3H, H_f) ppm. ^{13}C NMR (125 MHz, acetone-d_6): δ = 153.3, 153.2, 153.1 (4C, $C_{9,9',2,2'}$), 152.3 (1C, C_a), 151.5 (1C, C_h), 148.5, 148.3, 148.2, 148.1 (5C, $C_{10,10',11,11',g}$), 138.4 (1C, C_b), 137.0, 136.9, 136.6 (4C, $C_{4,4',7,7'}$), 131.1, 130.9, 130.6 (4C, $C_{12,12',13,13'}$), 128.2, 128.1, 127.9 (4C, $C_{5,5',6,6'}$), 126.9 (1C, C_e), 126.4 (2C, $C_{3,3'}$), 126.2 (1C,$C_{8'}$), 125.9 (1C,C_c), 125.5 (1C, C_8), 122.6 (C_d), 38.3 (C_f) ppm.

dx.doi.org/10.1021/ic5010598 | Inorg. Chem. 2014, 53, 8061−8070

■ ASSOCIATED CONTENT

Supporting Information

Crystallographic information files (CIF), all NMR data, UV−vis and PL titration data for complex **1**; characterization data for **1**[$H_2P_2O_7$]. This material is available free of charge via the Internetat http://pubs.acs.org. CCDC-990711 (**1**[$H_2P_2O_7$]) contains the supplementary crystallographic data for this paper.

■ AUTHOR INFORMATION

Corresponding Author

*E-mail: icpg@iacs.res.in.

Present Address

[§](S.K.) Centre for Advanced Studies in Chemistry, North Eastern Hill University, Shillong-793022, Meghalaya, India.

Notes

The authors declare no competing financial interest.

■ ACKNOWLEDGMENTS

Department of Science & Technology (DST), India, is greatly acknowledged for Swarnajayanti Fellowship to P.G., and B.C. thanks CSIR, India for fellowship (SRF). Single-crystal X-ray diffraction data of **1**[$H_2P_2O_7$] is collected at the DBT-funded CEIB program (Project No. BT/01/CEIB/11/V/13) awarded to Department of Organic Chemistry, IACS, Kolkata.

■ REFERENCES

(1) (a) Hirsch, A. K. H.; Fischer, F. R.; Diederich, F. *Angew. Chem., Int. Ed.* **2007**, *46*, 338−352. (b) Bowler, M. W.; Cliff, M. J.; Waltho, J. P.; Blackburn, G. M. *New J. Chem.* **2010**, *34*, 784−794.

(2) (a) Scenger, W. *Principles of Nucleic Acid Structure;* Springer: New York, 1998. (b) Le, D. H.; Kim, S. Y.; Hong, J. *Angew. Chem., Int. Ed.* **2004**, *43*, 4777−4780. (c) Katayev, E. A.; Ustynyuk, Y. A.; Sessler, J. L. *Coord. Chem. Rev.* **2006**, *250*, 3004−3037.

(3) (a) Schmidtchen, F. P.; Berger, M. *Chem. Rev.* **1997**, *97*, 1609−1646. (b) Beer, P. D.; Gale, P. A. *Angew. Chem., Int. Ed.* **2001**, *40*, 486−516.

(4) (a) Yoon, J.; Kim, S. K.; Singh, N. J.; Kim, K. S. *Chem. Soc. Rev.* **2006**, *35*, 355−360. (b) Steed, J. W. *Chem. Commun.* **2006**, 2637−2649. (c) Gale, P. A. *Chem. Commun.* **2011**, 82−86.

(5) (a) Sessler, J. L.; Gale, P. A.; Cho, W.-S. *Anion ReceptorChemistry;* RSC Publishing: Cambridge, U.K., 2006. (b) Kim, S.-K.; Lee, D.-H.; Hong, J.-I.; Yoon, J.-Y. *Acc. Chem. Res.* **2009**, *42*, 23−31. (c) Kumar, A.; Pandey, P. S. *Org. Lett.* **2008**, *10*, 165−168. (d) Chen, K.-H.; Liao, J.-H.; Chan, H.-Y.; Fang, J.-M. *J. Org. Chem.* **2009**, *74*, 895−898. (e) Xu, Z.; Singh, N. J.; Lim, J.; Pan, J.; Kim, H.-N.; Park, S.-S.; Kim, K. S.; Yoon, J.-Y. *J. Am. Chem. Soc.* **2009**, *131*, 15528−15533. (f) Oh, D. J.; Ahn, K. H. *Org. Lett.* **2008**, *10*, 3539−3542. (g) khatua, S.; Choi, S. H.; Lee, J.; Kim, K.; Do, Y.; Churchill, D. G. *Inorg. Chem.* **2009**, *48*, 2993−2999. (h) Das, P.; Bhattacharya, S.; Mishra, S.; Das, A. *Chem. Commun.* **2011**, *47*, 8118−8120. (i) Goswami, S.; Paul, S.; Manna, A. *RSC Adv.* **2013**, *3*, 10639−10643. (j) Kim, K.; Ha, Y.; Kaufman, L.; Churchill, D. G. *Inorg. Chem.* **2011**, *51*, 928−938. (k) Goswami, S.; Manna, A.; Paul, S.; Aich, K.; Das, A. K.; Chakraborty, S. *Dalton Trans.* **2013**, *42*, 8078−8085. (l) Kim, K. M.; Oh, D. J.; Ahn, K. H. *Chem.—Asian. J.* **2011**, *6*, 122−127. (m) Oh, D. J.; Kim, K. M.; Ahn, K. H. *Chem.—Asian. J.* **2011**, *6*, 2034−2039.

(6) (a) Sessler, J. L.; Cai, J.; Gong, H.-Y.; Yang, X.; Arambula, J. F.; Hay, B. P. *J. Am. Chem. Soc.* **2010**, *132*, 14058−14060. (b) Chen, K.-H.; Liao, J.-H.; Chan, H.-Y.; Fang, J.-M. *J. Org. Chem.* **2009**, *74*, 895−898. (c) Caballero, A.; Zapata, F.; González, L.; Molina, P.; Alkorta, I.; Elguero. *J. Chem. Commun.* **2014**, DOI: 10.1039/C4CC00169A. (d) Sokkalingam, P.; Kim, D. S.; Hwang, H.; Sessler, J. L.; Lee, C.-H. *Chem. Sci.* **2012**, *3*, 1819−1824. (e) For reviews, see: Sessler, J. L.; Davis, J. M. *Acc. Chem. Res.* **2001**, *34*, 989−997. (f) Sessler, J. L.; Camiolo, S.; Gale, P. A. *Coord. Chem. Rev.* **2003**, *240*, 17−55. (g) Lin, C.-I.; Selvi, S.; Fang, J.-M.; Kai, P.-T.; Chou, C. H.; Cheng, Y.-Y. *J. Org. Chem.* **2007**, *72*, 3537−3542. (h) Sessler, J. L.; Dan Pantos, G.; Gale, P. A. *Org. Lett.* **2006**, *8*, 1593−1596. (i) Gale, P. A. *Chem. Commun.* **2005**, 3761−3772. (j) Pfeffer, F. M.; Lim, K. F.; Sedgwick, K. J. *Org. Biomol. Chem.* **2007**, *5*, 1795−1799. (k) Chang, K.-J.; Moon, D.; Lah, M. S.; Jeong, K.-S. *Angew. Chem., Int.Ed.* **2005**, *44*, 7926−7929. (l) Causey, C. P.; Allen, W. E. *J. Org. Chem.* **2002**, *67*, 5963−5968. (m) Curiel, D.; Cowley, A.; Beer, P. D. *Chem. Commun.* **2005**, 236−238. (n) Cai, J.; Hay, B. P.; Young, N. J.; Yanga, X.; Gong, H.-Y.; Yang, X.; Sessler, J. L. *Chem. Sci.* **2013**, *4*, 1560−1567.

(7) (a) Haridas, V.; Lal, K.; Sharma, Y. K.; Upreti, S. *Org. Lett.* **2008**, *10*, 1645−1647. (b) Horne, W. S.; Yadav, M. K.; Scout, C. D.; Ghadiri, M. R. *J. Am. Chem. Soc.* **2004**, *126*, 15366−15367. (c) Li, Y.; Flood, A. H. *Angew. Chem., Int. Ed.* **2008**, *47*, 2649−2652. (d) Juwarker, H.; Lenhardt, J. M.; Pham, D. M.; Craig, S. L. *Angew. Chem., Int. Ed.* **2008**, *47*, 3740−3743. (e) Meudtner, R. M.; Hecht, S. *Angew.Chem., Int. Ed.* **2008**, *47*, 4926−4930. (f) Romero, T.; Caballero, A.; Tárraga, A.; Molina, P. *Org. Lett.* **2009**, *11*, 3466−3469. (g) Ornelas, C.; Aranzaes, J. R.; Cloutet, E.; Alves, S.; Astruc, D. *Angew. Chem., Int. Ed.* **2007**, *46*, 872−877.

(8) (a) Li, Y.; Flood, A. H. *J. Am. Chem. Soc.* **2008**, *130*, 12111−12122. (b) Bourne, Y.; Kolb, H. C.; Radic, Z.; Sharpless, K. B.; Taylor, P.; Marchot, P. *Proc. Natl. Acad. Sci. U.S.A.* **2004**, *101*, 1449−1454. (c) Bock, V. D.; Speijer, D.; Hiemstra, H.; Maarseveen, J. H. V. *Org. Biomol.Chem.* **2007**, *5*, 971−975. (d) Pokorski, J. K.; Jenkins, L. M.; Feng, M. H. Q.; Durell, S. R.; Bai, Y. W.; Appella, D. H. *Org. Lett.* **2007**, *9*, 2381−2383.

(9) (a) Nadler, A.; Hain, C.; Diederichsen, U. *Eur. J. Org. Chem.* **2009**, 4593−4599. (b) Schweinfurth, D.; Pattacini, R.; Strobel, S.; Sarkar, B. *Dalton Trans.* **2009**, 9291−9297. (c) Obata, M.; Kitamura, A.; Mori Kameyama, A. C.; Czaplewska, J. A.; Tanaka, R.; Kinoshita, I.; Kusumoto, T.; Hashimoto, H.; Harada, M.; Mikata, Y.; Funabiki, T.; Yano, S. *Dalton Trans.* **2008**, 3292−3300. (d) Schweinfurth, D.; Hardcastle, K. I.; Bunz, U. H. F. *Chem. Commun.* **2008**, 2203−2205. (e) Richardson, C.; Fitchett, C. M.; Keene, F. R.; Steel, P. J. *Dalton Trans.* **2008**, 2534−2537. (f) Meudtner, R. M.; Ostermeier, M.; Goddard, R.; Limberg, C.; Hecht, S. *Chem.—Eur. J.* **2007**, *13*, 9834−9840. (g) Huang, S.; Clark, R. J.; Zhu, L. *Org. Lett.* **2007**, *9*, 4999−5002.

(10) (a) Czarnik, A. W. *Acc. Chem. Res.* **1994**, *27*, 302−308. (b) Fabbrizzi, L.; Poggi, A. *Chem. Soc. Rev.* **1995**, 197−202. (c) Ojida, A.; Inoue, M.; Mito-oka, Y.; Hamachi, I. *J. Am. Chem. Soc.* **2003**, *125*, 10184−10185. (d) Gunnlaugsson, T.; Davis, A. P.; O'Brien, J. E.; Glynn, M. *Org. Lett.* **2002**, *4*, 2449−2452. (e) Valeur, B.; Leray, I. *Coord. Chem. Rev.* **2000**, *205*, 3−40. (f) Causey, C. P.; Allen, W. E. *J. Org. Chem.* **2002**, *67*, 5963−5968. (g) de Silva, A. P.; Vance, T. P.; West, M. E. S.; Wright, G. D. *Org. Biomol. Chem.* **2008**, *6*, 2468−2480. (h) Suksai, C.; Tuntulani, T. *Chem. Soc. Rev.* **2003**, *32*, 192−202. (i) Huang, X.; Guo, Z.; Zhu, W.; Xie, Y.; Tian, H. *Chem. Commun.* **2008**, 5143−5145. (j) Yoon, J.; Kim, S. K.; Singh, N. J.; Lee, J. W.; Yang, Y. J.; Chellappan, K.; Kim, K. S. *J. Org. Chem.* **2004**, *69*, 581−583. (k) Fabbrizzi, L.; Marcotte, N.; Stomeo, F.; Taglietti, A. *Angew. Chem., Int. Ed.* **2002**, *41*, 3811−3814. (l) Mizukami, S.; Nagano, T.; Urano, Y.; Odani, A.; Kikuchi, K. *J. Am. Chem. Soc.* **2002**, *124*, 3920−3925. (m) Zhang, J. F.; Kim, S.; Han, J. H.; Lee, S.-J.; Pradhan, T.; Cao, Q. Y.; Lee, S. J.; Kang, C.; Kim, J. S. *Org. Lett.* **2011**, *13*, 5294−5297. (n) Wu, F.-Y.; Li, Z.; Wen, Z.-C.; Zhou, N.; Zhao, Y.-F.; Jiang, Y.-B. *Org. Lett.* **2002**, *4*, 3203−3205.

(11) (a) Nazeeruddin, M. K.; Péchy, P.; Renouard, T.; Zakeeruddin, S. M.; Humphry-Baker, R.; Comte, P.; Liska, P.; Cevey, L.; Costa, E.; Shklover, V.; Spiccia, L.; Deacon, G. B.; Bignozzi, C. A.; Grätzel, M. *J. Am. Chem. Soc.* **2001**, *123*, 1613−1624. (b) Wang, P.; Klein, C.; Humphry-Baker, R.; Zakeeruddin, S. M.; Grätzel, M. *J. Am. Chem. Soc.* **2005**, *127*, 808−809. (c) Bessho, T.; Yoneda, E.; Yum, J.-H.; Guglielmi, M.; Tavernelli, I.; Imai, H.; Rothlisberger, U.; Nazeeruddin, M. K.; Grätzel, M. *J. Am. Chem. Soc.* **2009**, *131*, 5930−5934. (d) Hagfeldt, A.; Boschloo, G.; Sun, L.; Kloo, L.; Pettersson, H. *Chem. Rev.* **2010**, *110*, 6595−6663. (e) Robson, K. C. D.; Koivisto, B. D.; Yella, A.; Sporinova, B.; Nazeeruddin, K. M.; Baumgartner, T.; Grätzel, M.; Berlinguette, C. P. *Inorg. Chem.* **2011**, *50*, 5494−5508. (f) Badjic, J. D.; Ronconi, C. M.; Stoddart, J. F.; Balzani, V.; Silvi, S.; Credi, A. *J. Am. Chem. Soc.* **2006**, *128*, 1489−1499. (g) Petitjean, A.; Puntoriero, F.; Campagna, S.; Juris, A.;

Lehn, J. M. *Eur. J. Inorg. Chem.* **2006**, *19*, 3878−3892. (h) Balzani, V.; Bergamini, G.; Marchioni, F.; Ceroni, P. *Coord. Chem. Rev.* **2006**, *250*, 1254−1266. (i) Ozawa, H.; Haga, M.; Sakai, K. *J. Am. Chem. Soc.* **2006**, *128*, 4926−4927. (j) Meyer, T. J. *Nature* **2008**, *451*, 778−779. (k) Liu, F.; Concepcion, J. J.; Jurss, J. W.; Cardolaccia, T.; Templeton, J. L.; Meyer, T. J. *Inorg. Chem.* **2008**, *47*, 1727−1752. (l) Fan, Y.; Zhang, L.-Y.; Dai, F.-R.; Shi, L.-X.; Chen, Z.-N. *Inorg.Chem.* **2008**, *47*, 2811−2819. (m) Zhao, S.; Arachchige, S. M.; Slebodnick, C.; Brewer, K. J. *Inorg. Chem.* **2008**, *47*, 6144−6152. (n) Shiotsuka, M.; Nishiko, N.; Keyaki, K.; Nozaki, K. *Dalton Trans.* **2010**, *39*, 1831−1835. (o) Ozawa, H.; Sakai, K. *Chem. Commun.* **2011**, *47*, 2227−2242. (p) Hirahara, M.; Masaoka, S.; Sakai, K. *Dalton Trans.* **2011**, *40*, 3967−3978.

(12) (a) Schmittel, M.; Shu, Q. *Chem. Commun.* **2012**, *48*, 2707−2709. (b) Khatua, S.; Samanta, D.; Bats, J. W.; Schmittel, M. *Inorg. Chem.* **2012**, *51*, 7075−7086. (c) Khatua, S.; Schmittel, M. *Org. Lett.* **2013**, *15*, 4422−4425. (d) Zhang, P.; Pei, L.; Chen, Y.; Xu, W.; Lin, Q.; Wang, J.; Wu, J.; Shen, Y.; Ji, L.; Chao, H. *Chem.—Eur. J.* **2013**, *19*, 15494−15503.

(13) (a) Felici, M.; Contreras-Carballada, P.; Vida, Y.; Smits, J. M. M.; Nolte, R J. M.; Cola, L. D.; Williams, R. M.; Feiters, M. C. *Chem.—Eur. J.* **2009**, *15*, 13124−13134. (b) Collins, J. E.; Lamba, J. J. S.; Love, J. C.; McAlvin, J. E.; Ng, C.; Peters, B. P.; Wu, X.; Fraser, C. L. *Inorg. Chem.* **1989**, *38*, 2020−2024.

(14) (a) Maity, D.; Das, S.; Mardanya, S.; Baitalik, S. *Inorg. Chem.* **2013**, *52*, 6820−6838. (b) Maity, D.; Bhaumik, C.; Mondal, D.; Baitalik, S. *Inorg. Chem.* **2013**, *52*, 13941−13955.

(15) (a) Niu, H.-T.; Su, D.; Jiang, X.; Yang, W.; Yin, Z.; He, J.; Cheng, J.-P. *Org. Biomol. Chem.* **2008**, *6*, 3038. (b) Zhu, M.; Yuan, M.; Liu, X.; Lv, J.; Huang, C.; Liu, H.; Li, Y.; Wang, S.; Zhu, D. *Org. Lett.* **2008**, *10*, 1481.

(16) (a) Demas, J. N.; DeGraff, B. A. *Anal. Chem.* **1991**, *63*, 829A. (b) Lakowicz, J. R. *Principles of Fluorescence Spectroscopy,* 2nd ed.; Kluwer Academic/Plenum: New York, 1999.

(17) (a) Pyo, S.; Pérez-Cordero, E.; Bott, S. G.; Echegoyen, L. *Inorg. Chem.* **1999**, *38*, 3337−3343. (b) Baitalik, S.; Flörke, U.; Nag, K. *Inorg. Chem.* **1999**, *38*, 3296−3308. (c) Derossi, S.; Adams, H.; Ward, M. D. *Dalton Trans.* **2007**, 33−36. (d) Das, S.; Saha, D.; Bhaumik, C.; Dutta, S.; Baitalik, S. *Dalton Trans.* **2010**, *39*, 4162−4169. (e) Bhaumik, C.; Das, S.; Saha, D.; Dutta, S.; Baitalik, S. *Inorg. Chem.* **2010**, *49*, 5049−5062. (f) Saha, D.; Das, S.; Maity, D.; Dutta, S.; Baitalik, S. *Inorg. Chem.* **2011**, *50*, 46−61.

(18) (a) *SAINT and XPREP,* 5.1 ed.; Sheldrick, G. M., Ed.; Siemens Industrial Automation Inc.: Madison, WI, 1995. (b) *SADABS, Empirical Absorption Correction Program;* University of Göttingen: Göttingen, Germany, 1997.

(19) Sheldrick, G. M. *SHELXTL Reference Manual: Version 5.1;* Bruker AXS: Madison, WI, 1997.

(20) Sheldrick, G. M. *SHELXL-97: Program for Crystal Structure Refinement;* University of Göttingen: Göttingen, Germany, 1997.

(21) Spek, A. L. *PLATON-97;* University of Utrecht: Utrecht, The Netherlands, 1997.

(22) *Mercury 3.1* (supplied with Cambridge Structural Database); CCDC: Cambridge, U.K., 2003−2004.